

Construction of Ionic Liquid Self-assembled Monolayer on Gold Electrode for Hemoglobin Modifying and Peroxide Biosensing

Huamao Chen, Guangchao Zhao*

Anhui Key Laboratory of Chem-Biosensing, School of Chemistry and Materials Science, Anhui Normal University, Wuhu 241000, China

*E-mail: gczhao@mail.ahnu.edu.cn

Received: 20 October 2012 / Accepted: 17 November 2012 / Published: 1 December 2012

We constructed a self-assembled monolayer (SAM) of mercaptoacetic acid combining functionalized ionic liquid (IL-MAA) by covalent interaction on gold electrode. The formation of IL-MAA SAM on gold electrode has been confirmed by Fourier transform infrared spectroscopy (FT-IR), cyclic voltammetry (CV) and electrochemical impedance spectroscopy (EIS) in this article. The results of CV and EIS revealed that the electrochemical behavior of the $[\text{Fe}(\text{CN})_6]^{3-/4-}$ redox couple probe improved along with IL's introduction on gold electrode. As IL-MAA is electroactive, hemoglobin (Hb) was modified on the IL-MAA SAM gold electrode subsequently and the direct electrochemistry of Hb was realized. UV-vis spectrum illustrated that the Hb absorbed on the SAM film maintained its natural activity. Upon the optimal conditions, the modified electrode exhibited a high electrocatalytic activity to hydrogen peroxide. Accordingly, an easily-made and cost-effective hydrogen peroxide electrochemical biosensor, accompany with proper fine quality, was accomplished. More importantly, the methodology could provide an effective enzyme immobilization platform based on ionic liquid modifying electrode surface and broaden the use of functionalized ionic liquid in electrochemical biosensor field.

Keywords: Ionic liquid, Self-assembled monolayer, Hemoglobin, Electrocatalysis, Hydrogen peroxide

1. INTRODUCTION

Ionic liquid (IL) is currently receiving a great deal of attentions as novel media in chemistry and analytical chemistry [1, 2]. Providing an attractive combination of an electrochemical solvent and electrolyte, IL is playing an increasingly practical role in electrochemistry fields, which range from the laboratory bench to industrial manufacturing process [3]. Their advantages, including miniscule vapor pressure, high polarity, wide potential windows, relative inertness and universal biocompatibility, have also attract much attention in the fabrication and application of IL-based electrochemical sensors.

Several book chapter, perspective and review articles dealing with the application of IL in electrochemical biosensors are currently available [4-6]. There are three major strategies for developing proteins or enzymes based electrochemical biosensors. One is directly manufacturing so called carbon ionic liquid electrode (CILE) or carbon paste ionic liquid electrode (CPILE) [7, 8]. The other is modifying electrodes with IL or IL-based composites [9-13]. Another is providing IL as nonaqueous media for sensing application [14]. Nevertheless, there are still a lot of challenges in achieving IL-based easy-made, sensitive, selective, stable and reproducible biosensors for high speed analysis of biological and environmental compounds of interest.

Self-assembled monolayer (SAM) has been extensively used in recent years. The well-defined SAM films have already been proven to be extremely useful for incorporating redox couples into electrochemical interfaces and exploring protein adsorption [15, 16]. This technique is expected to yield preparation easy, highly versatile, controllable and stable approach for tailoring electrode surfaces. Accordingly, a number of remarkable accounts on biosensors or electrochemical biosensors through SAM methods blossom [17, 18]. For example, Wang had used SAM in several kinds of DNA sensing [19]. And a series of immunosensing methods based on SAM were carried out for immunoassay [20, 21]. Besides, determination of dopamine at N-acetylcysteine SAM modified gold electrodes and simultaneous determination of epinephrine and ascorbic acid at triazole SAM modified gold electrodes were also reported [22]. In addition, Cortina-Puig et al proposed an amperometric cytochrome c based sensor for the determination of the antioxidant capacity of pure substances alliin extracted from garlic bulbs and natural samples. In that method, cytochrome c and xanthine oxidase enzyme were co-immobilized on the gold screen-printed electrode using the combination of several long-chain thiols [23]. Additionally, hemoglobin was also immobilized onto a stable SAM of thiolated-viologen (V_8SH) and used to design H_2O_2 biosensor. The sensor offered an excellent electrochemical response for H_2O_2 concentration below the μmol level with high sensitivity and selectivity according to the report [24]. Mai et al studied the electrochemical behaviors of hemoglobin by adsorbing Hb on gold electrodes modified with SAMs of $HS(CH_2)_nCOOH$ ($n= 1, 2, 5, 10$). They found that the hydrocarbon chain length influences the direct electro transfer of Hb [25]. Nevertheless, the SAM of IL, which was used for the fabrication of biosensor, could be scarcely seen.

Recently, more attention has been paid on IL participated SAM. In the published documents, octadodecanethiol SAM on gold electrode in 1-butyl-3-methylimidazolium hexafluorophosphate was stable in a much wider potential window than in organic electrolyte and other aqueous solutions [26]. Some thiol-functionalized and triethoxysilyl-functionalized imidazolium ILs can also form SAMs on gold and Si/SiO₂ substrate surfaces respectively [27, 28]. And yet, many SAMs, especially those molecules with long carbon chains size, tend to influence monolayer coverage resulting in the lower biomolecule immobilization efficiency and block the electrotransfer between the redox species and the underlying electrode. While short molecules lead to poor assembly and (poor) stability under sensing conditions [29, 30]. Thus, to find proper molecules or graft different molecules in constructing SAM systems is essential. For this reason, Xu et al integrated humic acid with cysteamine SAM film for cytochrome c deposition on the modified electrodes [31]. In another paper, SAM of IL 1-(12-mercaptododecyl)-3-methylimidazolium bromide on Au could be tuned by changing the deposition temperature and improved the electron transfer property for neutral and negatively charged redox

mediators [32]. Although several kinds of thiol-functionalized IL had been synthesized and studied in SAM system, the synthesis and purification together with low productivity are still challenge of sensor and biosensor field. Therefore, an investigation to understand the intrinsic redox behavior of the protein in SAM of IL and construct electrochemical biosensor are still required. As far as we known, there is few paper of Hb adsorbed on SAM of IL that has been published till date.

Here, we combined a kind of hydroxyl-functionalized imidazole-based IL (1-(2-hydroxyethyl)-3-methylimidazolium tetrafluoroborate) onto mercaptoacetic acid (MAA) SAM on gold by covalent conjunction through a simple chemical reaction procedure. As a result, a stable IL-MAA SAM layer was obtained on gold electrode surface. The obtained IL SAM averted the sophisticated synthesis and purification procedure. Subsequently, Hb was adsorbed on the modified gold electrode and the direct electrochemistry of Hb was realized. For the application of the electrode, an Hb-based electrochemical biosensor for H_2O_2 determination was accomplished. The IL-MAA SAM could enhance the adsorption of Hb, give mild conditions to retain the bioactivity of Hb and promote its electron transfer rate. The fabricated H_2O_2 biosensor exhibited satisfactory results of wide linear range, low limit of detection, stability and fast response.

2. EXPERIMENTAL

2.1. Chemicals and materials

Hb was obtained from Sigma Chemical Company and used without further purification. The 2 mg mL^{-1} Hb stock solutions were prepared by pH 7.0 phosphate buffer solutions (PBS, 0.1 M) and stored at temperature of 4 °C. Hydroxyl-functionalized ionic liquid (1-(2-hydroxyethyl)-3-methylimidazolium tetrafluoroborate) was synthesized according to the literature [33]. The products were characterized by NMR and IR and the results were accordance with the literature. Concentrated sulfuric acid (H_2SO_4 , 98.3%) and hydrogen peroxide solutions (H_2O_2 , 30.0%) were purchased from Sinopharm Chemical Reagent Co. Ltd. (Shanghai, china). All other chemicals were of analytical grade and used as obtained. A fresh deoxygenated stock ethanol solution of 5 mM MAA was prepared each day before the modification. Stock solutions of H_2O_2 were diluted from 30% solution. PBS (0.1 M) with various pH values were prepared by mixing standard stock solutions of K_2HPO_4 (0.1 M) and NaH_2PO_4 (0.1 M) to proper pH. All solutions were made up with double distilled water.

2.2. Apparatus and measurements

The electrochemical measurements were carried out on a conventional three-electrode cell system with a computer-controlled CHI 660B electrochemical workstation (CH Instruments, USA). The polycrystalline gold electrode with 2 mm diameter or the modified electrodes were used as the working electrodes and a platinum spiral wire as the counter electrode. All potentials were referred to Ag/AgCl electrode (KCl-saturated) unless stated otherwise. The electrochemical impedance spectra (EIS) measurements were performed in the presence of 5.0 mM $\text{K}_3[\text{Fe}(\text{CN})_6]/\text{K}_4[\text{Fe}(\text{CN})_6]$ (1:1)

mixture as a redox probe prepared in 0.1 M KCl solution. EIS were recorded at the bias potential equal to the redox probe's formal potential (0.18 V) applying 5 mV AC voltage in the frequency range of 0.05 Hz - 100 kHz and plotted in the form of complex plane diagrams (Nyquist plots). The electrolyte for electrochemical measurements was purged with high purity nitrogen for at least 30 min prior to measurements. Then the electrochemical cell was kept under nitrogen atmosphere throughout the experiments. All experiments were carried out at room temperature. Infrared spectroscopic characterization was carried out on a FTIR-8400S Fourier transform infrared spectroscopy (Shimadzu, Japan) with wavelength range of 500 - 3,800 cm^{-1} . UV-vis reflection and absorption spectra measurements were recorded on a UV-2450 UV-vis spectrophotometer (Shimadzu, Japan) with wavelength range of 300 - 500 nm.

2.3. Preparation of SAM modified gold electrodes

The bare gold electrode was first polished carefully with alumina slurry (0.05 μm) on microcloth to mirror and sonicated in double distilled water and ethanol, and then cleaned by a piranha (7:3 ratio of conc H_2SO_4 and 30% H_2O_2) solution. It was subsequently treated by cycling between potential windows of -0.3 V and +1.5 V versus Ag/AgCl in a 0.5 M H_2SO_4 solution at a scan rate of 0.1 V s^{-1} , until reproducible scan results were obtained. Then the cleaned electrode was thoroughly rinsed with distilled water for use. The real surface area (A_r) of the electrochemically activated gold electrode could be calculated by integrating the current beneath the cathodic wave of the cyclic voltammograms obtained in 0.5 M H_2SO_4 solution on the basis of the quantity of consumed charge 482 $\mu\text{C cm}^{-2}$ [34]. According to the ratio of the real surface area (A_r) to the geometrical area (A_g), the high roughness factor ($r_f = A_r / A_g$) of 3.75 in average was obtained, which implied the adequate activation of the bare gold electrode [35].

The SAM layer of IL-MAA was obtained by a simple in-situ esterification reaction between hydroxyl-functionalized IL and carboxyl group containing MAA SAM layer. Briefly, the pretreated clean gold electrode was first immersed in 5 mM deoxygenated MAA ethanol solution for 12 h at 4 $^\circ\text{C}$ in darkness. The resulting MAA monolayer-modified electrode was rinsed thoroughly with water and soaked in deoxygenated water for 12 h to remove the physically adsorbed MAA. Then, it was dried quickly with nitrogen atmosphere flow and dipped into a 1:1 mixture of IL with concentrated sulfuric acid at 80 $^\circ\text{C}$ under nitrogen blowing for agitation. After 24 h, an IL-MAA SAM modified gold electrode was obtained, which was noted as IL-MAA/Au. Immobilization of Hb on IL-MAA/Au surfaces was achieved through a dip-coating and phase-inversion method. The IL-MAA modified gold electrode was dipped into 2 mg ml^{-1} Hb solution for 12 h at 4 $^\circ\text{C}$. In such a way, a modified gold electrode Hb/IL-MAA/Au was obtained. For comparison, Hb/Au and Hb/MAA/Au electrodes were prepared in the same procedure except that bare gold electrode and MAA modified gold electrode were used respectively. All the resulting electrodes were washed with water and stored in pH 7.0 PBS at 4 $^\circ\text{C}$ for use.

3. RESULTS AND DISCUSSION

3.1. Surface characterization of the modified electrodes

The formation of SAM layer on gold electrode via the S-Au bond can be confirmed by the electrochemical desorption experiment [36]. Reductive desorption of the modified Au electrode was carried out in a degassed 0.5 M KOH solution. This reductive desorption of thiol-SAM on the Au surface is a one-electron reaction process. The surface concentration of the thiolates on MAA SAM can therefore be roughly determined from the charge consumed during the reductive desorption. The modified gold electrode exhibits a voltammetric response with a cathodic wave at -1.13 ± 0.01 V, which is due to the reductive desorption of the surface-attached MAA thiolates. By integrating the current under the cathodic wave, the estimated surface coverage for the MAA is $(5.6 \pm 0.3) \times 10^{-10}$ mol cm^{-2} . The surface coverage for IL-MAA was nearly the same as that of MAA, which mean that the graft of IL scarcely destroyed the SAM of MAA. The results pledged the stability of modified gold electrode and further application in the biosensor.

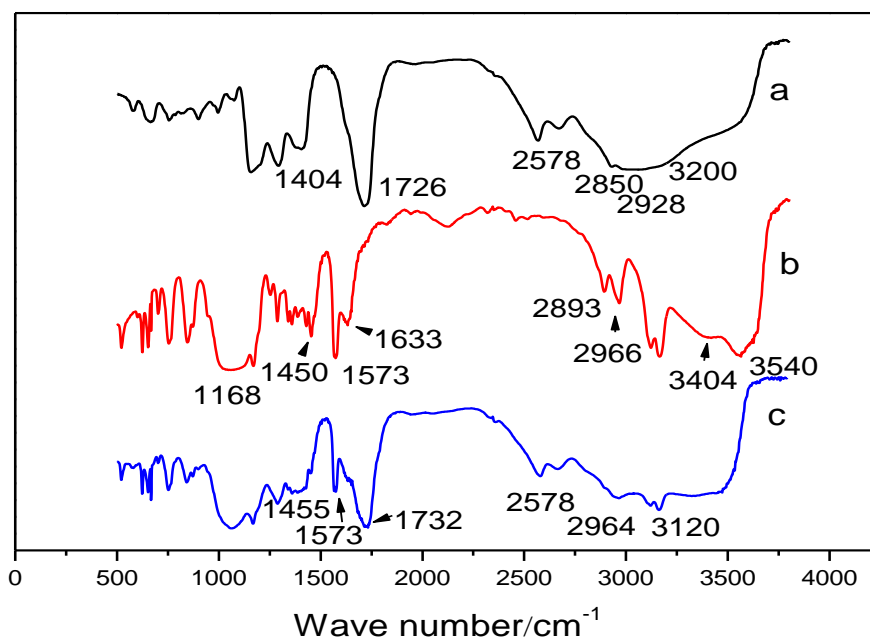


Figure 1. FT-IR spectra of (a) MAA, (b) IL and (c) IL-MAA SAM modified electrode.

The successful conjunction of IL with the MAA SAM can be further confirmed from the FT-IR characterizations. Figure 1 shows the FT-IR spectra (KBr) of MAA (a), IL (b) and IL-MAA (c). The spectra were shifted downward for easy viewing. The presence of Au-S at ~ 2578 cm^{-1} in the spectrums of both a and c indicated the form of SAM on gold. The spectrum of MAA in Figure 1a illustrates O-H ($\nu(\text{carboxyl})$) at ~ 1404 cm^{-1} , O-H (broad coupling $\nu(\text{O-H})$) at ~ 3200 cm^{-1} originated from carboxylic acid, C=O in carboxyl group at ~ 1726 cm^{-1} . Obvious absorbance bands of the asymmetric and symmetric CH_2 stretching vibrations of the assembled MAA locate at ~ 2928 cm^{-1} and ~ 2850 cm^{-1} ,

respectively. The spectrum of IL in Figure 1b, which was almost conform to the literature [33], was confirmed. That is, the presence of the O-H at 3404 cm^{-1} (while the band at $\sim 3540\text{ cm}^{-1}$ could be due to the O-H stretching mode of intercalated water), the C-H stretching bands located at 2966 cm^{-1} and 2893 cm^{-1} , C-O vibration at 1060 cm^{-1} and the C-H vibration at $\sim 1450\text{ cm}^{-1}$, as well as the imidazolium framework vibration at 1633 cm^{-1} ($\nu(\text{C}=\text{N})$), 1573 cm^{-1} ($\nu(\text{C}=\text{C})$) and 1168 cm^{-1} ($\nu(\text{C}-\text{N})$) are primarily evidenced. In figure 1c, the bands at 1732 cm^{-1} is the evidence of ester group. While the absorbance bands of O-H in IL and MAA disappeared. The lost of characteristic peaks of hydroxyl groups and the present bands of ester group confirmed that the esterification reactions between the IL and the MAA had been finished and the IL-MAA SAM formed successfully. The FT-IR spectrum of IL-MAA also exhibits IL features, which are the presence of the C-H stretching bands located at about 3120 cm^{-1} and 2964 cm^{-1} , and the C-H vibration at 1455 cm^{-1} , as well as the imidazolium framework vibration at 1632 cm^{-1} and 1573 cm^{-1} .

Electrochemical impedance spectroscopy (EIS) can give information on the impedance changes of the electrode surface during the modification process. The EIS include a semicircle part and a linear part. The semicircle part at higher frequencies corresponds to the electron-transfer limited process, the semicircle diameter of EIS equals to the electron transfer resistance (R_{et}), which controls the electron transfer kinetics of the redox probe at the electrode interface. And the linear part at lower frequencies corresponds to the diffusion process. Curve a in Figure 2 (A) shows the Nyquist plot of the EIS obtained at bare Au electrode. The R_{et} for bare Au electrode is lower than $15\ \Omega$ because of the good conductivity of gold. The EIS of the MAA SAM showed a higher R_{et} ($335\ \Omega$, Figure 2 (A), curve b), indicating that the MAA monolayer obstructed electron transfer of the electrochemical probe. Smaller R_{et} ($198\ \Omega$, Figure 2(A), curve c) was found when IL grafted the MAA modified gold electrode. This should be ascribed to the effective electro transfer promotion effect of IL. As the density of attached molecules and their orientation impact the impedance by hindering current flow across the electrode/electrolyte interface [37]. The particular orientation of the newly built IL-MAA on the gold electrode surface may build up a network, which could effectively improve heterogeneous electron transfer kinetics between the redox couple and electrode interface. Besides, the electrostatic attraction between the positively charged IL and the negatively charged probe ions may play a part. The R_{et} the Hb/IL-MAA modified electrode increased significantly ($800\ \Omega$, Figure 2 (A), curve d) due to the insulated polypeptide backbone of Hb obstacle the electron transfer of the probe. The result indicates that Hb can be adsorbed on the surface of IL-MAA modified electrode and results in the remarkable increase of surface negative charges [38]. All these results also show that Hb and IL-MAA were successfully assembled on the gold electrode surface and formed a tunable kinetic barrier, which is consistent with the subsequent voltammetry results.

Cyclic voltammetry of an electroactive species such as $[\text{Fe}(\text{CN})_6]^{3-/4-}$ is a valuable tool for testing the kinetic barrier of the interface. The extent of kinetic hindrance to the electron transfer process increases with the increasing thickness and the decreasing defect density of the barrier. Figure 2 (B) compares the CV responses of a bare Au electrode with that of a MAA/Au electrode, an IL-MAA/Au electrode and an Hb/IL-MAA/Au electrode in 5.0 mM ferri/ferrocyanide couple (1:1) with 0.1 M KCl solution. A pair of well-defined cyclic voltammograms with a peak-to-peak potential separation (ΔE_p) of 0.084 V was observed at the bare Au electrode (Figure 2 (B), curve a). After

modified with MAA SAM, the peak current decreased evidently and the ΔE_p increased prodigiously to 0.246 V (Figure 2 (B), curve b), showing the MAA SAM could obstacle the electron transfer of ferricyanide to gold electrode. While at the IL-MAA/Au (Figure 2 (B), curve c), the peak current increased obviously, which was larger than both bare Au electrode and MAA modified electrode, together with the ΔE_p decreased (0.072 V). The smaller ΔE_p and larger peak currents in curve c of Figure 2 (B) suggested that the IL-MAA SAM layer could enhance the electron transfer rate of $[\text{Fe}(\text{CN})_6]^{3-/4-}$.

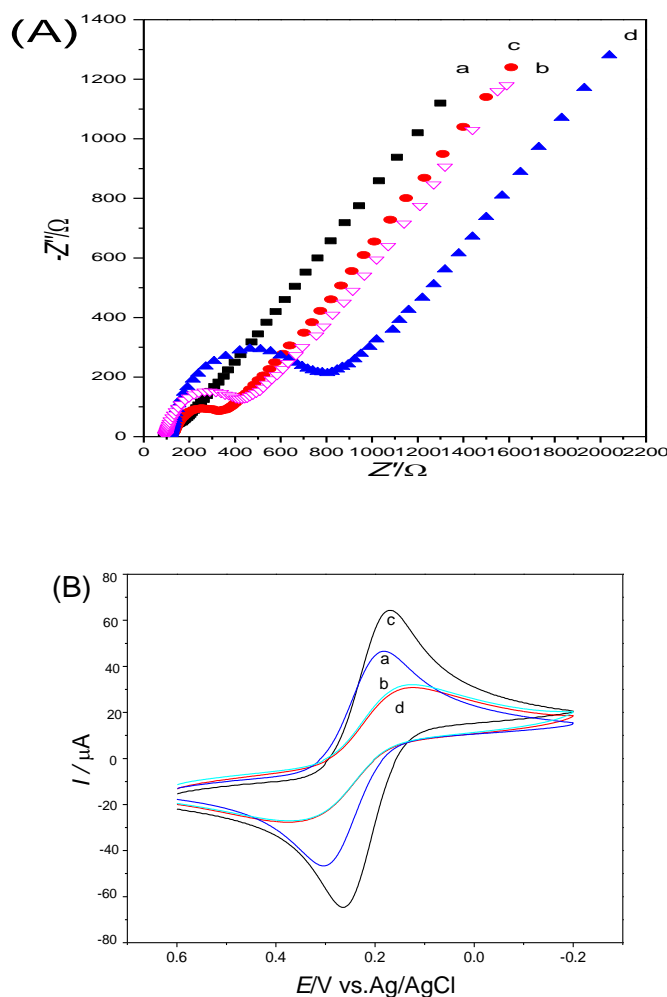


Figure 2. (A) The electrochemical impedance spectroscopy of (a) bare Au, (b) MAA/Au, (c) IL-MAA/Au and (d) Hb/IL-MAA/Au electrodes in the presence of 5.0 mM $\text{K}_3[\text{Fe}(\text{CN})_6]/\text{K}_4[\text{Fe}(\text{CN})_6]$ (1:1) and 0.1 M KCl solution. (B) CVs of (a) bare Au, (b) MAA/Au, (c) IL-MAA/Au, (d) Hb/IL-MAA/Au electrodes in the presence of 5.0 mM $\text{K}_3[\text{Fe}(\text{CN})_6]/\text{K}_4[\text{Fe}(\text{CN})_6]$ (1:1) containing 0.1 M KCl solution at scan rate of 100 mV s^{-1} .

This should ascribe to the good conductivity of IL, which could enhance the charge transfer through pinhole or electronic tunnel of SAM between the modifying layer and substrate gold electrode. Although the increase of peak currents was partly due to the effect of preconcentration of hexacyanoferrates on IL, the surface charge had none drastic effect on ΔE_p [39]. Thus, the smaller ΔE_p and larger peak currents was on account of the introduction of IL. Moreover, the attached

protein/enzyme often had the similar negative charge as $[\text{Fe}(\text{CN})_6]^{3-/4-}$ ions. Accordingly, the results indicated that IL-MAA SAM could effectively enhance the electrocatalytic activity and had potential using in electroanalysis and electrochemical biosensor field. When Hb was introduced (Figure 2 (B), curve d), the peak current lose and the ΔE_p decrease dramatically (0.223 V), which was due to the block of Hb between the probe ions and the electrode surface.

3.2. Characteristics of Hb in SAM

UV-vis absorption spectrum is useful conformational probe for heme proteins, which may provide information about possible denaturation of heme proteins. When Hb was denaturation, the locations of the Soret absorption band of iron heme shifted or disappeared [40]. The UV-vis spectrum of Hb film shows a Soret band at 406 nm (Figure 3 a). Figure 3 c displays the Soret band of Hb immobilized on an IL-MAA modified electrode. Its Soret absorption band is very close to that of pure Hb, which illustrates that the Hb molecule possessed the similar secondary structure as the native state of Hb and maintained its biological activity at its immobilized state. The difference of only 2 nm observed also confirmed the interaction between Hb and IL-MAA SAM layer.

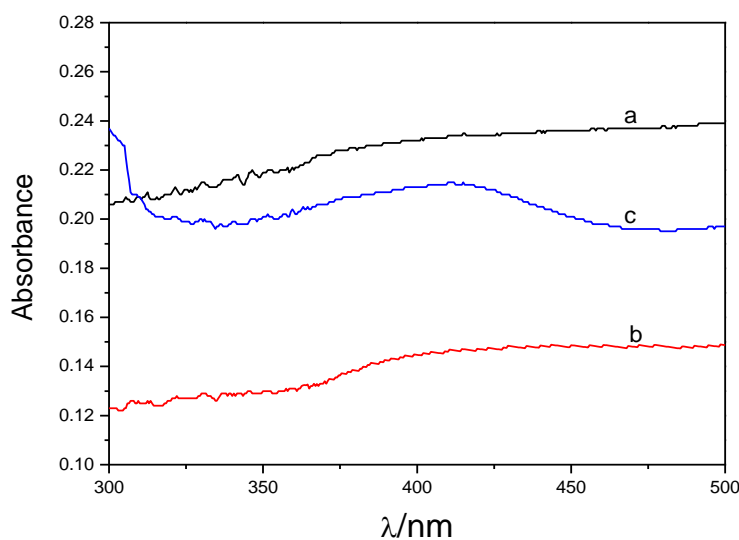


Figure 3. UV-vis absorption spectra of (a) Hb, (b) IL-MAA film and (c) Hb/IL-MAA film on modified electrode. The absorbance coordinate reflects only relative absorbance.

3.3. Direct electrochemistry of Hb/IL-MAA/Au electrode

Hemoglobin is one of the most used proteins in electrochemical studies. It is a metalloprotein found in red blood cells and it functions as an oxygen carrier of blood. Hb ($\text{MW} = 64,500 \text{ g mol}^{-1}$) contains four electro-active iron hemes as prosthetic groups in its respective four polypeptide chains. These redox centers serve as oxygen-binding sites on the molecule so Hb is a model system for studying electron transfer reactions in biological systems. However, it is difficult to obtain direct

electron transfer between Hb and an electrode because prosthetic groups are deeply buried inside the protein. Unfavorable orientation on the electrode surface increases the distance between heme-electrode surface and also adsorption of denatured protein on the bare electrode causes slow heterogeneous electron transfer rate. The fabricated IL-MAA SAM gold electrode is an effective way to enhance the electron transfer. Figure 4 (A) exhibited the variant direct electrochemistry of Hb on bare Au electrode (a), MAA/Au (b) and IL-MAA/Au (c) in PBS (pH 7.0). There is no obvious response of Hb on bare Au electrode probably because of the denaturation of Hb on gold. On the SAM of MAA, Hb showed a weak current response, which was in accordance with the reported results [25], implying MAA was serviceable for the direct electrochemistry of Hb. While on the IL-MAA SAM gold electrode the cyclic voltammogram exhibited well-defined redox peaks. Because of the positive excess charge of IL accumulated at the interface, the system could effectively immobilize Hb by electrostatic interaction. On the other hand, the newly built IL-MAA layer showed good biocompatible properties and maintained the natural structure of Hb on the modified electrode. In addition, the stable modification of IL-MAA on gold electrode pledged the direct electro transfer between Hb and the underlying electrode. As a result, the IL-MAA layer undertook an efficient electro transfer promoter or mediator between Hb and Au electrode.

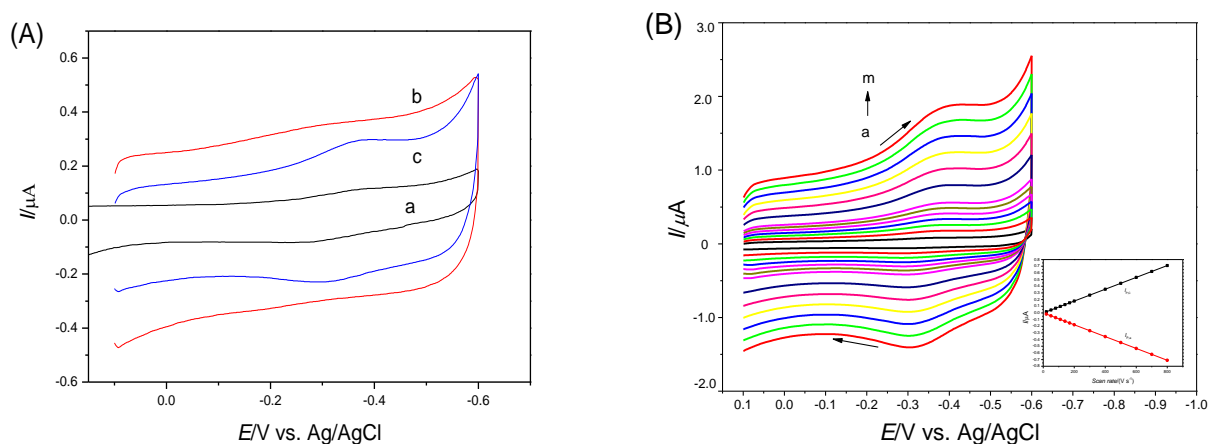


Figure 4. (A) Cyclic voltammograms of (a) Hb/Au, (b) Hb/MAA/Au and (c) Hb/IL-MAA/Au electrodes in 0.1 M PBS (pH 7.0) at scan rate of 100 $mV s^{-1}$. (B) Cyclic voltammograms of the Hb/IL-MAA/Au electrode in 0.1 M PBS (pH 7.0) at scan rates of 20, 50, 80, 110, 140, 170, 200, 300, 400, 500, 600, 700 and 800 $mV s^{-1}$ (a-h) respectively. Inset: the plots of cathodic and anodic peak current vs. scan rate.

Figure 4 (B) gives the typical cyclic voltammograms of the Hb/IL-MAA/Au electrode in pH 7.0 PBS with scan rates from 0.02 to 0.80 $V s^{-1}$. Nearly symmetric cathodic and anodic peaks of approximately equal height for Hb were obtained. With the increase of the scan rate, the redox peak currents increased simultaneously. As shown in the inset of Figure 4 (B), the cathodic and anodic peak currents ($I_{p,c}$ and $I_{p,a}$) are linear with scan rates from 0.02 to 0.80 $V s^{-1}$. The cathodic and anodic ΔE_p is ca. 66 mV and the formal potential (E^0) of Hb is -0.332 V. The ΔE_p is almost independence on the scan rate as indicated for quasi-reversible redox behavior. All these results are characteristics of

diffusionless, surface-controlled electrochemical process, which is similar to a chitosan-IL, surfactant or clay modified hemoglobin film electrodes [41]. According to the integrals of the reduction peaks and Laviron's equation [42]:

$$I_p = \frac{n^2 F^2 A \Gamma^* \nu}{4RT} = \frac{nFQ}{4RT}$$

Where Γ^* is the average surface coverage of the electron reaction substance (mol cm^{-2}). A is the electrode area (cm^2) and Q is the quantity of charge (C), calculated from the peak area of the voltammograms. The symbols n , I_p , F , R and T have their usual meanings. From the slope of the I_p - ν curve, n was calculated to be 0.9. Therefore, the redox of Hb on an IL-MAA modified gold electrode is a single electron transfer reaction. The average surface coverage (Γ^*) of Hb immobilized was calculated to be $4.49 \times 10^{-11} \text{ mol cm}^{-2}$, indicating a monolayer of Hb participated in the electron transfer process on the surface of electrode, which is approximately close to the theoretical monolayer coverage of Hb ($1.89 \times 10^{-11} \text{ mol cm}^{-2}$) [43].

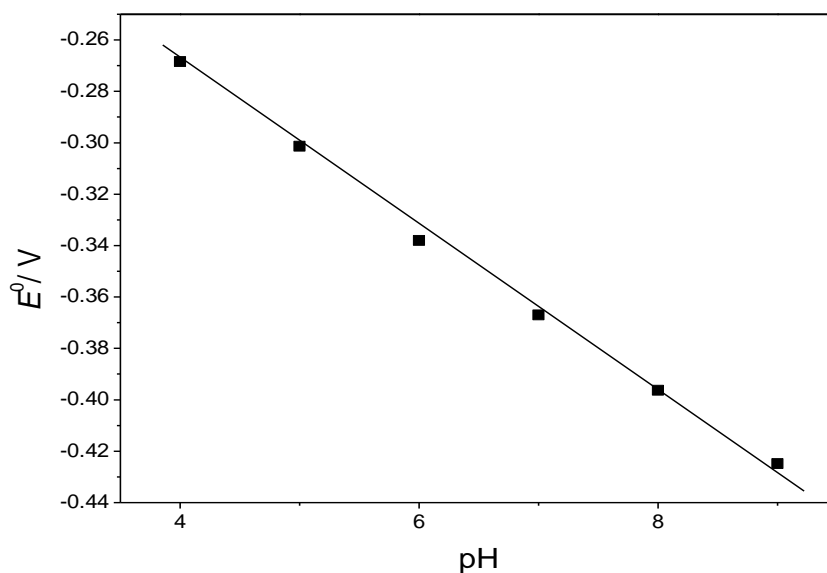


Figure 5. Dependence of pH values on formal potentials of the Hb/IL-MAA/Au electrode.

Supposing the charge transfer coefficient was between 0.3 and 0.7, the electron transfer rate constant (k_s) was estimated to be 1.98 s^{-1} according to Laviron's model with the formula $k_s = mnF\nu/RT$ [44], where m is a parameter related to ΔE_p . This value is higher than that of Hb on V_8SH (V_8SH : thiolated-viologen) (0.89 s^{-1}) [24], mercaptopropionic acid SAM (0.49 s^{-1}) [25], and GNSs/APTES/ITO (GNSs: gold nanoshells, APTES: 3-aminopropyltrimethoxysilane, ITO: indium tin oxide electrode) ($2.39 \pm 0.7 \text{ s}^{-1}$) [38], and at the Hb/GNPs/cystamine/Au electrode (0.49 s^{-1}) as reported previously [45]. The fast k_s indicating a reasonably fast electron transfer between Hb and the immobilized gold electrode should ascribe to the presence of IL-MAA SAM layer.

The effect of pH was also investigated at a pH range of 4.0 to 9.0. The direct electrochemistry of Hb/IL-MAA/Au electrode showed strong dependence on solution pH (figure 5). Negative shifts were obtained both in the oxidation and reduction peak potentials with the increase of pH value. There was a linear relationship between E° and the pH values with a slope of -38.0 mV pH^{-1} for the modified electrode. The slope value is smaller than the theoretical value of -58.0 mV pH^{-1} at $20 \text{ }^{\circ}\text{C}$ for the electron transfer accompanied with an equal number of protons in electrode reaction [46]. This could be attributed to the influence of the protonation states of trans ligands to the heme iron and amino acids around Hb, or the protonation of water molecule coordinated to the central iron [47]. Redox peak currents were also affected by pH change. Maximum peak currents were obtained at pH 7.0 indicating Hb had its highest bioactivity around pH 7.0 which is similar to the earlier literature [48].

3.4. Electrocatalysis of Hb/IL-MAA/Au to H_2O_2

According to the previous reports, it was shown that Hb shows peroxidase activity for the catalysis of reduction of H_2O_2 . With the addition and increasing concentration of H_2O_2 in 0.1 M PBS, an increase in the cathodic peak current and a decrease in the anodic peak current for Hb at the Hb/IL-MAA/Au electrode were observed (Figure 6 (A)), showing an obvious catalytic reaction process. The disappearance of anodic peak showed that the oxidation rate of Hb by H_2O_2 is very fast. However, comparing with the cyclic voltammograms in the presence of H_2O_2 at the Hb/IL-MAA/Au electrode, no reduction peak changes at bare Au electrode and slightly changes at MAA modified gold electrode were seen (Figure 6 (B)). All these results illustrated that the pseudo peroxidase bioelectrocatalytic activity of Hb on the IL-MAA SAM layer maintained well and further verified that the immobilized Hb retained its essential secondary structure. The efficient electrocatalytic effect should be ascribed to the assistant of the electro-active and stable IL-SAM layer.

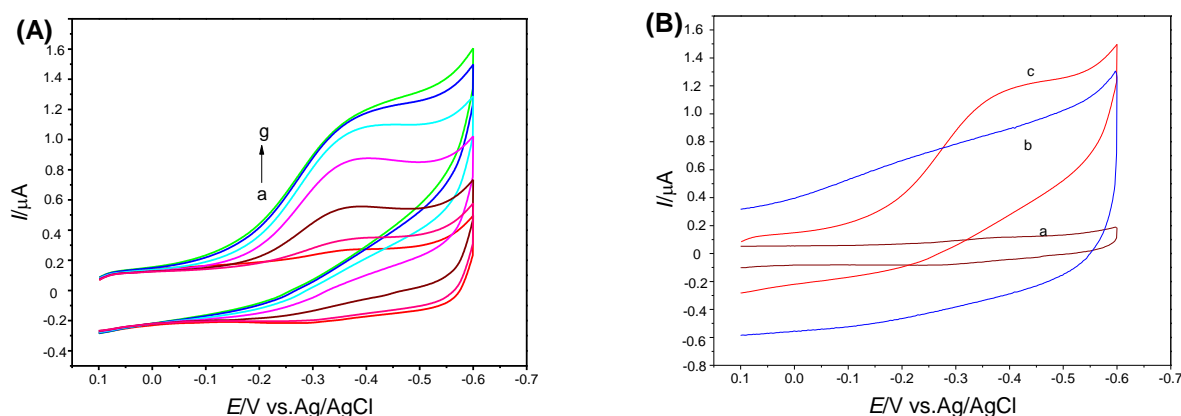


Figure 6. (A) Cyclic voltammograms of the Hb/IL-MAA/Au electrode at scan rate of 100 mV s^{-1} in 0.1 M PBS (pH 7.0) containing (a) 0 μM , (b) 6.25 μM , (c) 31.25 μM , (d) 68.75 μM , (e) 106.25 μM , (f) 143.75 μM and (g) 181.25 μM H_2O_2 . (B) Comparing Cyclic voltammograms of (a) Hb/Au, (b) Hb/MAA/Au and (c) Hb/IL-MAA/Au electrodes at scan rate of 100 mV s^{-1} in 0.1 M PBS (pH 7.0) with 100 μM H_2O_2 .

Electrocatalytic reduction of H_2O_2 using Hb/IL-MAA/Au electrode was further studied by amperometry which is one of the most commonly used technique for H_2O_2 sensing. Figure 7 depicted typical current-time relationship of the biosensor to H_2O_2 in 0.1 M PBS (pH 7.0) at an applied potential of -0.33 V upon successive additions of H_2O_2 in the time intervals of 20 s. After successive additions of H_2O_2 in PBS, the amperometric response increased linearly in the concentration range from 6.25×10^{-6} M to 4.75×10^{-4} M with a correlation coefficient of 0.999 (Figure 7 inset). The limit of detection (LOD) was calculated to be 4.68×10^{-7} M (based on the $S/N=3$) and the response time required to reach 95% of stable current response was ~ 0.6 sec. The performances of the prepared biosensor were favorable compared with some previous H_2O_2 biosensors in Table 1 owing to its broad linear concentration range and low LOD.

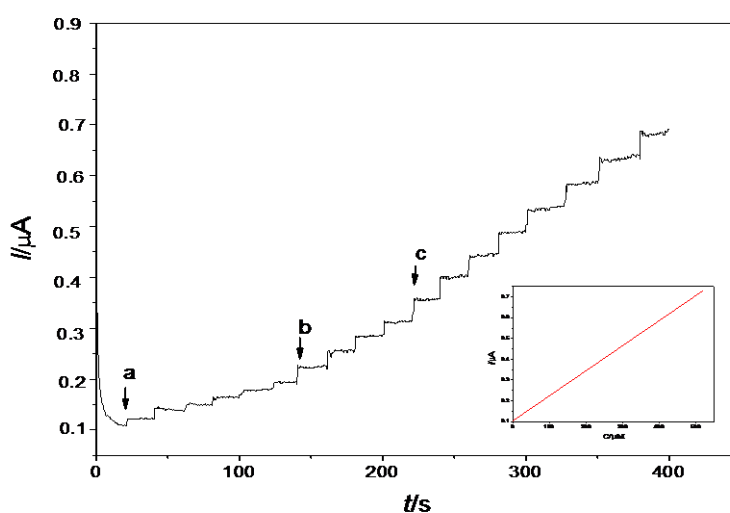


Figure 7. Typical Amperometric response of the biosensor to H_2O_2 in 0.1 M PBS (pH 7.0) at an applied potential of -0.33 V upon successive additions of (a) 12.5 μM , (b) 25 μM and (c) 37.5 μM H_2O_2 in the time intervals of 20 s. (Insert: The calibration curve of the biosensor.)

Table 1. Comparison of Various types of Hb-based-modified electrodes for H_2O_2 determination

Electrode ^a	Linear range (μM)	Limit of detection (μM)	References
Hb/ $\text{V}_8\text{SH}/\text{Au}$	10-125	0.25	[24]
Hb/GNSs/APTES/ITO	5-1000	3.4	[38]
Hb/MPPA/3D-Au	0.078-91	0.025	[46]
Hb/ZnO-MWCNTs/Nafion	0.2-12	0.084	[47]
Hb/PANI/MPA/Au	7.4-127	4.6	[48]
Hb/TNT-C/GC	1-100	0.92	[49]
Hb/Cht-Aus/Cys/Au	13-740	6.4	[50]
Hb/PC/PG	10-100	3.9	[51]
Hb/silica sol-gel/CPE	1.0-280	0.86	[52]
Hb/DNA/Au	25-125	0.4	[53]
Hb/IL-MAA/Au	6.25-475	0.47	This work

Note a: GNSs, gold nanoshells; APTES, 3-aminopropyltrimethoxysilane; ITO, indium tin oxide; MPPA, 3-mercaptopropylphosphonic acid; MWCNTs, multiwalled carbon nanotubes; PANI, polyaniline; MPA, 3-mercaptopropanoic acid; TNT-C, carbonized TiO₂ nanotubes; Cht-Aus, chitosan-stabilized gold nanoparticle; Cys, cysteine; PC, egg phosphatidylcholine; PG, pyrolytic graphite; CPE, carbon paste electrode.

The catalytic peak current also showed characteristics of Michaelis-Menten kinetics. The apparent Michaelis-Menten constant K_m^{app} , which gives an indication of the enzyme-substrate kinetics, can be calculated according to Lineweaver-Burk equation $\frac{1}{I_{ss}} = \frac{1}{I_{max}} + \frac{K_m^{app}}{I_{max}C}$ [54]. Where I_{ss} is the net catalytic steady state current in solution at certain concentration of H₂O₂, I_{max} is the net maximum catalytic peak current in the calibration plot, C stand for the bulk concentration of H₂O₂ in solution. It is well known that a smaller K_m^{app} represents a higher catalytic ability. The K_m^{app} in this work is 28.8 μM, which is much lower than 87.5 μM for Hb on Carbonized TiO₂ nanotubes [49], 120 μM obtained at Hb/GNPs/cysteamine/Au [51], 180 μM at Hb/GNSs/APTES/ITO [38], 0.31 mM at Hb/ZrO₂/DMSO/PG [55], 1.4 mM at Hb/Cht-Aus/Cys/Au [50], and 0.2 mM at Cyt c/nano-LTL-zeolite/ITO electrode [56]. The smaller apparent Michaelis-Menten constant implied that Hb immobilized on IL-MAA SAM showed higher affinity and activity to H₂O₂ substrate.

3.5. Analysis property of Hb/IL-MAA/Au to H₂O₂

The reproducibility of the biosensor was illustrated by three independent experimental cycles. A relative standard deviation (RSD) of 2.25% (n=5) at 50 μM H₂O₂ concentration was found, which implied that the electrode had a good reproducibility. The repeatability of the sensor for current response was examined too. The biosensor was found to have good repeatability with the RSD of 3.65% for ten successive measurements at a H₂O₂ concentration of 50 μM. After 2 weeks of storage period in PBS (pH 7.0) at 4 °C, the modified gold electrode retained about 94% of its initial amperometric response to H₂O₂. All the results showed that the established biosensor has exhibited good reproducibility and stability.

The interference effect of some substances on the amperometric response of H₂O₂ was examined to test the selectivity of the biosensor. The current inhibition was obtained for each interfering substance presenting at a concentration of 0.50 mM. The results showed that glucose, acetic acid, ethanol, citric acid and uric acid did not cause any observable interference in the detection of 50 μM H₂O₂. But in the case of ascorbic acid, the response currents decreased by 25% from their respective initial values. The effect was presumably due to the consumption of H₂O₂ by the oxidation of ascorbic acid.

4. CONCLUSIONS

In conclusion, a thin layer modification of gold electrode with IL-MAA by self-assembled method is feasible. The SAM proved to be stable and efficient for promoting the fast electron transfer

of Hb and showed a good adsorption capability for Hb. These characteristics, along with its fine combination properties make the sensor promising for the amperometric determination of H₂O₂.

The preparation easy, highly versatile and stable approach for tailoring electrode surfaces provide universal reference frame. On the one hand, the designed IL-MAA SAM modified electrode has the potential applications in simultaneous determination of inorganic species or bioactive molecules. The further work about this is carrying out in our lab. On the other hand, in-situ preparation of IL and modifying electrode provide a simple and practical method of electrode modification. Since ionic liquid can be designed to maintain different kinds of task-specific group attached to the ionic liquid framework. According to the mentality, many kinds of functionalized ionic liquid can be fabricated onto the corresponding electrodes in the similar way. Thus, the work demonstrates a new avenue of functionalization of ionic liquid and will play a part in sensing and biosensing field.

ACKNOWLEDGEMENT

This project was supported by the National Natural Science Foundation of China. (Grant No. 20975001)

References

1. S. Lee, *Chem. Commun.*, 11 (2006) 1049.
2. J. P. Hallett, T. Welton, *Chem. Rev.*, 111 (2011) 3508.
3. M. B. Pomfret, D. J. Brown, A. Epshteyn, A. P. Purdy, J. C. Owrutsky, *Chem. Mater.*, 20 (2008) 5945.
4. N. J. Ronkainen, H. B. Halsall, W. R. Heineman, *Chem. Soc. Rev.*, 39 (2010) 1747.
5. M. J. A. Shiddiky, A. A. J. Torriero, *Biosens. Bioelectron.*, 26(2011) 1775.
6. M. Opallo, A. Lesniewski, *J. Electroanal. Chem.*, 656 (2011) 2.
7. A. Safavi, N. Maleki, O. Moradlou, M. Sorouri, *Electrochem. Commun.*, 10 (2008) 420.
8. Z. Zhu, L. Qu, Q. Niu, Y. Zeng, W. Sun, X. Huang, *Biosens. Bioelectron.*, 26 (2011) 2119.
9. G. -C. Zhao, M. -Q. Xu, J. Ma, X. -W. Wei, *Electrochem. Commun.*, 9 (2007) 920.
10. E. Zapp, D. Brondani, I. C. Vieira, J. Dupont, C. W. Scheeren, *Electroanalysis*, 23 (2011) 1124.
11. H. Chen, G. Zhao, *J. Solid State Electrochem.*, 16 (2012) 3289.
12. K. Liu, J. Zhang, G. Yang, C. Wang, J. -J. Zhu, *Electrochem. Commun.*, 12 (2010) 402.
13. S. Dong, P. Zhang, H. Liu, N. Li, T. Huang, *Biosens. Bioelectron.*, 26 (2011) 4082.
14. H. Y. Xiong, T. Chen, X. H. Zhang, S. F. Wang, *Electrochem. Commun.*, 9 (2007) 2671.
15. S. Q. Lud, M. Steenackers, P. Bruno, D. M. Gruen, P. Feulner, J. A. Garrido, M. Stutzmann, M. Stutzmann, *J. Am. Chem. Soc.*, 128 (2006) 16884.
16. K. Prime, G. Whitesides, *Science*, 252 (1991) 1164.
17. D. Samanta, A. Sarkar, *Chem. Soc. Rev.*, 40 (2011) 2567.
18. E. Asav, E. Akyilmaz, *Biosens. Bioelectron.*, 25 (2010) 1014.
19. Y. Wang, C. J. Li, X. H. Li, Y. F. Li, H. B. Kraatz, *Anal. Chem.*, 80 (2008) 2255.
20. S. K. Mwilu, A. O. Aluoch, S. Miller, P. Wong, O. A. Sadik, *Anal. Chem.*, 81 (2009) 7561.
21. Md. M. Billah, C. S. Hodges, H. C.W. Hays, P.A. Millner, *Bioelectrochem.*, 80 (2010) 49.
22. Y. -X. Sun, S. -F. Wang, X. -H. Zhang, Y. -F. Huang, *Sensor. Actuat. B-Chem.*, 113 (2006) 156.
23. M. Cortina-Puig, X. Muñoz-Berbel, C. Calas-Blanchard, J. -L. Marty, *Talanta*, 79 (2009) 289.
24. A. K. M. Kafi, D. -Y. Lee, S. -H. Park, Y. -S. Kwon, *Microchem. J.*, 85 (2007) 308.
25. Z. Mai, X. Zhao, Z. Dai, X. Zou, *Talanta*, 81 (2010) 167.
26. J. Li, Y. Shen, Y. Zhang, Y. Liu, *Chem. Commun.*, 3 (2005) 360.

27. B. S. Lee, Y. S. Chi, J. K. Lee, I. S. Choi, C. E. Song, U. K. Namgoong, S. -g. Lee, *J. Am. Chem. Soc.*, 126 (2004) 480.
28. Y. S. Chi, S. Hwang, B. S. Lee, J. Kwak, I. S. Choi, S. -g. Lee, *Langmuir*, 21 (2005) 4268.
29. R. K. Mendes, R. F. Carvalhal, L. T. Kubota, *J. Electroanal. Chem.*, 612 (2008) 164.
30. O. Seitz, P. G. Fernandes, R. Tian, N. Karnik, H. -C. Wen, H. Stiegler, R. A. Chapman, E. M. Vogel, Y. J. Chabal, *J. Mater. Chem.*, 21 (2011) 4384.
31. J. -J. Xu, G. Wang, Q. Zhang, D. -M. Zhou, H. -Y. Chen, *Electrochem. Commun.*, 6 (2004) 278.
32. M. Branca, D. Correia-Ledo, O. R. Bolduc, M. Ratel, A. R. Schmitzer, J. -F. Masson, *Phys. Chem. Chem. Phys.*, 13 (2011) 12015.
33. S. H. Yeon, K. S. Kim, S. Choi, H. Lee, H. S. Kim, H. Kim, *Electrochim. Acta.*, 50 (2005) 5399.
34. Y. Chen, L. -R. Guo, W. Chen, X. -J. Yang, B. Jin, L. Min, *Bioelectrochem.*, 75 (2009) 26.
35. Urs Oesch, Jiří Janata, *Electrochim. Acta*, 28 (1983) 1237.
36. S. Zhang, L. Echegoyen., *J. Am. Chem. Soc.*, 127 (2005) 2006.
37. J. Wu, D. M. Crokek, A. C. West, S. Banta, *Anal. Chem.*, 82 (2010) 8235.
38. Y. Wang, W. Qian, Y. Tan, S. Ding, H. Zhang, *Talanta*, 72 (2007) 1134.
39. S. Alwarappan, A. Erdem, C. Liu, C. Z. Li, *J. Phys. Chem. C*, 113 (2009) 8853.
40. A. -E. F. Nassar, W. S. Willis, J. F. Rusling, *Anal. Chem.*, 67 (1995) 2386.
41. Y. L. Zhou, N. F. Hu, Y. H. Zeng, J. F. Rusling, *Langmuir*, 18 (2002) 211.
42. E. Laviron, *J. Electroanal. Chem.*, 100 (1979) 263.
43. D. D. Schlereth, *J. Electroanal. Chem.*, 646 (1999) 198
44. E. Laviron, *J. Electroanal. Chem.*, 101 (1979) 19.
45. H. Y. Gu, A. M. Yu, H. Y. Chen, *J. Electroanal. Chem.*, 516 (2001) 119.
46. Y. Chen, X. J. Yang, L. R. Guo, J. Li, X. H. Xia, L. M. Zheng, *Anal. Chim. Acta*, 644 (2009) 83.
47. W. Ma, D. Tian, *Bioelectrochem.*, 78 (2010) 106.
48. G. Bolat, F. Kuralay, S. Abaci, *Chem. Senses.*, 2 (2012) 1.
49. C. Guo, F. Hu, C. M. Li, P. K. Shen, *Biosens. Bioelectron.*, 24 (2008) 819.
50. J. J. Feng, G. Zhao, J. J. Xu, H. Y. Chen, *Anal. Biochem.*, 342 (2005) 280.
51. X. Han, W. Huang, J. Jia, S. Dong, E. Wang, *Biosens. Bioelectron.*, 17 (2002) 741.
52. Q. Wang, G. Li, B. Yang, *Sensor. Actuator. B-Chem.*, 99 (2004) 50.
53. A. K. M. Kafi, F. Yin, H. -K. Shin, Y. -S. Kwon, *Thin Solid Films*, 499 (2006) 420.
54. R. A. Kamin, G. S. Wilson, *Anal. Chem.*, 52 (1980) 1198.
55. X. Lu, Q. Zhang, L. Zhang, J. Li, *Electrochem. Commun.*, 8 (2006) 874.
56. T. Yu, Y. Zhang, C. You, J. Zhuang, B. Wang, B. Liu, Y. Kang, Y. Tang, *Chem. Eur. J.*, 12 (2006) 1137.